Single crystal growth and characterization of $HfS_{2(1-x)}Se_{2x}$ ternary alloys

Cheng-Wen Wang[1], Der-Yuh Lin[1], Hung-Pin Hsu[2]

[1] Department of Electronic Engineering, National Changhua University of Education,
No.2, Shi-Da Road, Changhua City, Changhua County 500, Taiwan
Phone: +886-4-723-2105-8337 E-mail: dylin@cc.ncue.edu.tw
[2] Department of Electronic Engineering, Ming Chi University of Technology,
No.84, Gongzhuan Road, Taishan District, New Taipei City 243, Taiwan

Abstract

New two-dimensional materials such as HfS_2 and $HfSe_2$ crystals are attracting research attention owing to the great potential for electronic and optoelectronic applications. In this study, we reported the single crystal growth and characterizations of $HfS_{2(1-x)}Se_{2x}$ (x= 0, 0.2, 0.6, 1) ternary alloys including their crystal parameters and optical properties. We synthesized HfS_2, $HfS_{0.8}Se_{1.2}$, $HfS_{1.6}Se_{0.4}$ and $HfSe_2$ single crystals by using chemical vapor transport (CVT) method and using iodine as a transport agent. The surface morphology has been examined by scanning electron microscope (SEM) and the elemental compositions have been verified by energy dispersive X-ray spectroscopy (EDS) and electron probe microanalyzer (EPMA), the crystal structure has been determined by X-Ray diffraction (XRD) and high resolution transmission electron microscope (HR-TEM). Raman scattering spectra show that the change of phonon peaks for various compositions. We also have performed the absorption measurements at the temperatures of 300 K to investigate the band gap energies of $HfS_{2(1-x)}Se_{2x}$ ternary alloys.

1. Introduction

HfS_2 is one of the novel two dimensional (2D) transition metal dichalcogenides (TMDCs). It could be an ideal sustainable energy electronic material, and it also has the value of application of optoelectronic components. The energy gap of HfS_2 is slightly larger than 1 eV (1.23 eV), which is close to that of silicon (1.12 eV), and is also an indirect energy gap semiconductor. Moreover, its oxide has a high dielectric constant, even higher than that of SiO_2. So, HfS_2 has the potential to be a good candidate for realizing low power devices. HfSe2 is an emerging 2D material with very high electron mobility (~3500 $cm^2V^{-1}s^{-1}$) and has been fabricated as a top-gated transistor with native high dielectric constant oxide (HfO_2). It is also nice thermoelectric material with low lattice thermal conductivity and can be used for thermoelectric applications. By tuning the composition ratio of these two materials, the engineering of modulating energy gap can be performed to provide great flexibility for the design of optoelectronic components and create promising heterostructure of new TMDCs. $HfS_{2(1-x)}Se_{2x}$ ternary alloys have the exhibit compositionally tunable optical properties and electronic structures. Thus, 2D ternary semiconductors attract lots of research interest due to their appreciable band gaps in optical and electrical properties.

In this study, we changed the proportion of S components in HfS_2 and added Se, through chemical vapor transport method, grew four different compounds of $HfS_{2(1-x)}Se_{2x}$ ternary alloys. Consequently, we analyze the lattice structures by XRD and HR-TEM technologies. The HR-TEM images reveal a random arrangement of the S and Se atoms in the 2D alloys. We also measure the optical properties of $HfS_{2(1-x)}Se_{2x}$ alloys by absorption spectra to determine their band gap energies. The dependence between the lattice constants and composition has been studied. Furthermore, the band gap energies for various compositions and the bowing parameter are studied.

2. Results and discussions

Figure 1(a) shows the XRD patterns for $HfS_{2(1-x)}Se_{2x}$ alloys with different Se contents. As show in Figure 1, we observed only (002) diffraction peak of $HfSe_2$, $HfS_{0.8}Se_{1.2}$, $HfS_{1.6}Se_{0.4}$, and HfS_2 at 2θ = 29.08, 29.7, 30.23 and 30.6. As expected, the main peak positions of $HfS_{2(1-x)}Se_{2x}$ alloys gradually shift toward high angles with increasing S content in Figure 1. Using the eq.(1) and eq.(2) and assuming λ =1.5406 Å, we can obtain the lattice constants of c for these four samples are 6.136 Å, 6.011 Å, 5.913 Å, and 5.838 Å. Moreover, all of the peaks are derived from the direction of c-axis, which strongly points out that the crystals have nice single crystalline nature. Vegard's law can describe the relationship between the crystal lattice constant of these alloys and the concentrations of the constituent elements.

$$2d_{hkl} \sin\theta = n\lambda \qquad (1)$$

$$\frac{1}{d^2_{hkl}} = \frac{4}{3}\left(\frac{h^2+hk+k^2}{a^2}\right) + \frac{l^2}{c^2} \qquad (2)$$

The Raman peaks reveal the phonon energies result from the vibration of atomic S-Hf-S and Se-Hf-Se. The signal E_{1g} is generated by the vibration of Hf and S (Se) in the direction of the xy layered plane, and the A_{1g} comes from the vibration in the direction of the z-axis. Figure 1(b) shows the A_{1g} mode of $HfSe_2$ locates at 200.1 cm^{-1} and shifts to 334.3 cm^{-1} for HfS_2. While the E_{1g} mode of $HfSe_2$ is found at 148.4 cm^{-1} and shifts to 258 cm^{-1} for HfS_2. This result indicates the increase of sulfur composition will increase the phonon vibration energy due to the decrease of the lattice constants.

The HR-TEM image presented in figure 2(a) clearly reveals a naked view of hexagonal structured lattice, which

with good consistency to the atomic model of $HfS_{0.8}Se_{1.2}$ with hexagonal order of Hf, S and Se. The obtained lattice plane spacing from figure 2(a) is 0.368 nm. Figure 2(b) shows the pattern of selected area electron diffraction (SAED) measurement which reveals a six-fold symmetry and confirms the single crystallinity of $HfS_{0.8}Se_{1.2}$. We get lattice constant of a by SAED with different Se composition, and show the results in Table 1. Because the radius of Se atoms is larger than that of S atoms, the lattice constants of a and c increase with the increasing Se composition.

Figure 3(a) shows the SEM image of the $HfS_{1.6}Se_{0.4}$ crystals, which clearly indicates a layered structure. It exhibits a unique crystal structure with stacking layers that act via weak van der waals force between neighboring layers. As shown in the SEM and EDS results, the smooth surface of $HfS_{1.6}Se_{0.4}$ with obvious layer structures and uniform distribution of lead and iodide elements indicate the good quality of $HfS_{1.6}Se_{0.4}$ crystals. The composition x measured by EDS has been listed in Table 2. The result is consistent to the composition of source materials.

Figure 4(a) shows the absorption spectra of the $HfS_{2(1-x)}Se_{2x}$ crystals measured at 300 K. From the absorption spectra, the band gap energies can be determined from the extrapolation of the linear least squares fit of $\alpha^{1/2}$ to the baselines indicated by the dotted lines. The results are listed in Table 2. The band gap energy decreases from 2.04 eV (HfS_2) to 1.21 eV ($HfSe_2$) with the increase of Se content at 300 K. This result demonstrated that the band gap energies can be tuned with variation of Se composition. The result can be indicated by the conventional bowing parameter, as described in eq. (3):

$$E_g(x) = xE_g(SnSe_2) + (1-x)E_g(SnS_2) - bx(1-x) \quad (3)$$

where the band gap bowing parameter b was calculated to be of 0.50 eV.

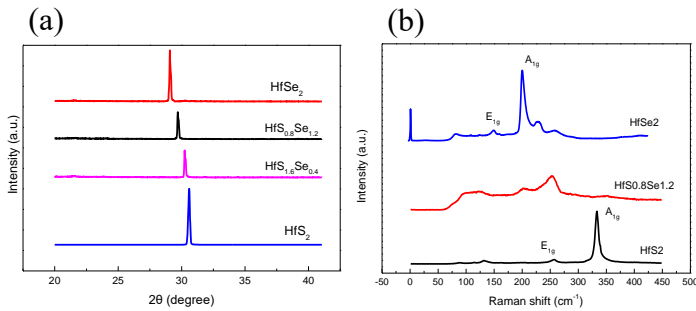shows the lattice constant calculated to be 0.368 nm), and (b) SAED pattern (right) of bulk

Figure 3 (a) SEM image of bulk $HfS_{1.6}S_{0.4}$ (b) EDS image of bulk $HfS_{1.6}S_{0.4}$

Table 1 Compositions lattice parameter c and a of $HfS_{2(1-x)}Se_{2x}$ alloys

x value in $HfS_{2(1-x)}Se_{2x}$	c (Å)	a (Å)	c/a
1	6.136	3.77	1.627
0.6	6.011	3.72	1.615
0.2	5.913	3.68	1.606
0	5.838	3.64	1.603

Figure 4 (a) Absorption spectra of $HfS_{2(1-x)}Se_{2x}$ alloys with four different Se compositions (x = 0, 0.2, 0.6, and 1, respectively), and (b) composition-dependent band-gaps and the corresponding fitting curve of $HfS_{2(1-x)}Se_{2x}$ alloys

Table 2 Compositions bandgap of $HfS_{2(1-x)}Se_{2x}$ at 300K, and EDS analysis of different Se content

x value in $HfS_{2(1-x)}Se_{2x}$	Band gap energy at 300K (eV)	x value (measures by EDS)
1	1.21	0.92
0.6	1.48	0.56
0.2	1.72	0.22
0	2.04	0

3. Conclusions

We have grown a series of $HfS_{2(1-x)}Se_{2x}$ ternary alloy bulk crystals with four different Se compositions by using CVT method. We presented the crystal structure by XRD, HR-TEM, SEM and Raman spectra. We also conducted the optical studies of absorption measurements. According to the measurement results we observed obviously that red shift behavior of the indirect bandgap by increasing the Se Content. It means that the bandgap are changed with different Se composition. The band-gap bowing parameter b was calculated by absorption spectra, with value of 0.50 eV. Therefore, we can know that the application of optoelectronic devices can be extended by controllable doping band gap engineering.

Fig. 1 (a) $HfS_{2(1-x)}Se_{2x}$ alloys XRD with different Se contents, and (b) raman spectrum of bulk $HfS_{2(1-x)}Se_{2x}$

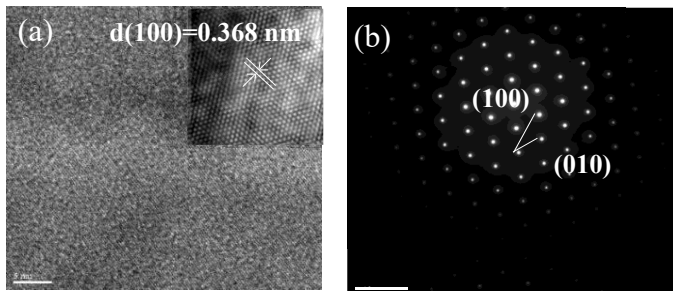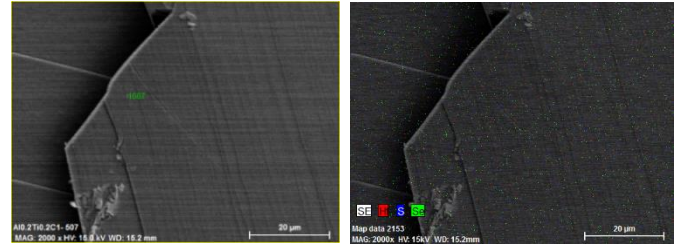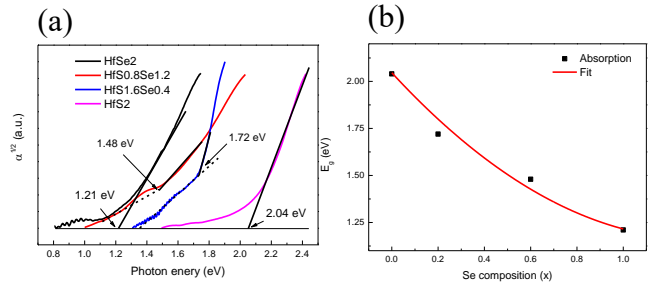Figure 2 (a) HR-TEM image of bulk $HfS_{0.8}S_{1.2}$ (inset above